Biochimica et Biophysica Acta 1788 (2009) 732–742

Contents lists available at ScienceDirect

Biochimica et Biophysica Acta

journal homepage: www.elsevier.com/locate/bbamem

Infrared spectroscopy studies of mixtures prepared with synthetic ceramides varying in head group architecture: Coexistence of liquid and crystalline phases

M. Janssens, G.S. Gooris, J.A. Bouwstra *

Leiden/Amsterdam Center for Drug Research, Department of Drug Delivery Technology, Gorlaeus Laboratories, Leiden University, P.O. Box 9502, 2300 RA Leiden, The Netherlands

ARTICLE INFO

Article history:
Received 8 October 2008
Received in revised form 1 December 2008
Accepted 13 January 2009
Available online 21 January 2009

Keywords:
Ceramides
Skin
Lipid organization
Infrared spectroscopy
Stratum corneum

ABSTRACT

The barrier function of the skin is provided by the stratum corneum (SC), the outermost layer of the skin. Ceramides (CERs), cholesterol (CHOL) and free fatty acids (FFAs) are present in SC and form highly ordered crystalline lipid lamellae. These lamellae are crucial for a proper skin barrier function. In the present study, Fourier transform infrared spectroscopy was used to examine the lipid organization of mixtures prepared from synthetic CERs with CHOL and FFAs. The conformational ordering and lateral packing of these mixtures showed great similarities to the lipid organization in SC and lipid mixtures prepared with native CERs. Therefore, mixtures with synthetic CERs serve as an excellent tool for studying the effect of molecular architecture of CER subclasses on the lipid phase behavior. In SC the number of OH-groups in the head groups of CER subclasses varies. Furthermore, acylCERs with a linoleic acid chemically bound to a long acyl chain are also identified. The present study revealed that CER head group architecture affects the lateral packing and conformational ordering of the CER:CHOL:FFA mixtures. Furthermore, while the majority of the lipids form a crystalline packing, the linoleate moiety of the acylCERs participates in a "pseudo fluid" phase.

1. Introduction

The primary function of the skin is to serve as an interface in order to control the influences from the environment. As the skin acts as a permeability barrier, it also reduces water loss from the body and therefore helps to control processes in the skin. The permeability barrier is located in the outermost layer of the skin, the stratum corneum (SC). The SC mainly consists of dead cells (corneocytes) surrounded by an extracellular lipid matrix. In human SC approximately 15–20 layers of dead cells are present. The structure of the SC is often compared to that of a brick wall. The bricks are formed by the corneocytes, while the lipid matrix is the mortar between the cells. The corneocytes are almost impermeable for compounds and the lipid regions are the only continuous structure in SC. For this reason the transport of substances (including drugs) applied onto the skin is mainly directed along the tortuous pathway of the intercellular lipid regions [1,2]. This demonstrates that the hydrophobic lipids are considered to play a crucial role in the barrier function of the skin. It is well-known that the SC lipids form highly ordered crystalline lamellae running approximately parallel to the skin surface [3,4]. A detailed knowledge about lipid composition and organization is of great importance for understanding the barrier function in normal skin and the impaired barrier function in diseased skin. In the SC of diseased skin often a change in lipid composition is encountered.

The composition of the SC lipids is very exceptional, as phospholipids are nearly absent. The major lipid classes in SC are ceramides (CERs), cholesterol (CHOL) and free fatty acids (FFAs). The FFAs mainly consist of saturated chains with a length varying between 16 and 26 carbon atoms. The most abundant chain lengths are 22 and 24 carbon atoms in length [5]. At least 9 different subclasses of CERs have been identified in human SC. The CERs differ from each other by their head group architecture and acyl chain length [6].

Although CERs are abundantly present in SC, these lipid classes are also present in living cell membranes and may play a role in the raft formation. Especially the interactions between CER and CHOL are of interest in this raft formation.

In previous studies Fourier transform infrared spectroscopy (FTIR), electron diffraction and X-ray diffraction have been used for the detailed study of the lipid organization in SC [7–13]. These studies revealed that in human SC two lamellar phases coexist with repeat distances of approximately 6 nm and 13 nm, referred to as the short periodicity phase (SPP) and the long periodicity phase (LPP), respectively. It has been suggested that the LPP plays an important role in the barrier function of the skin [14]. Additional studies have shown that the lateral packing of the lipids is mainly orthorhombic. These studies also revealed that a small population of lipids most probably forms a hexagonal and/or a liquid lateral packing [15–17]. The presence of crystalline phases at high CHOL levels is very exceptional in lipid mixtures [18–21], which may contribute to the

* Corresponding author. Leiden/Amsterdam Center for Drug Research, Department of Drug Delivery Technology, Leiden University, P.O. Box 9502, Einsteinweg 55, 2333 CC Leiden, The Netherlands. Tel.: +31 71 5274219; fax: +31 71 5274565.
E-mail address: bouwstra@chem.leidenuniv.nl (J.A. Bouwstra).

0005-2736/$ – see front matter © 2009 Elsevier B.V. All rights reserved.
doi:10.1016/j.bbamem.2009.01.003

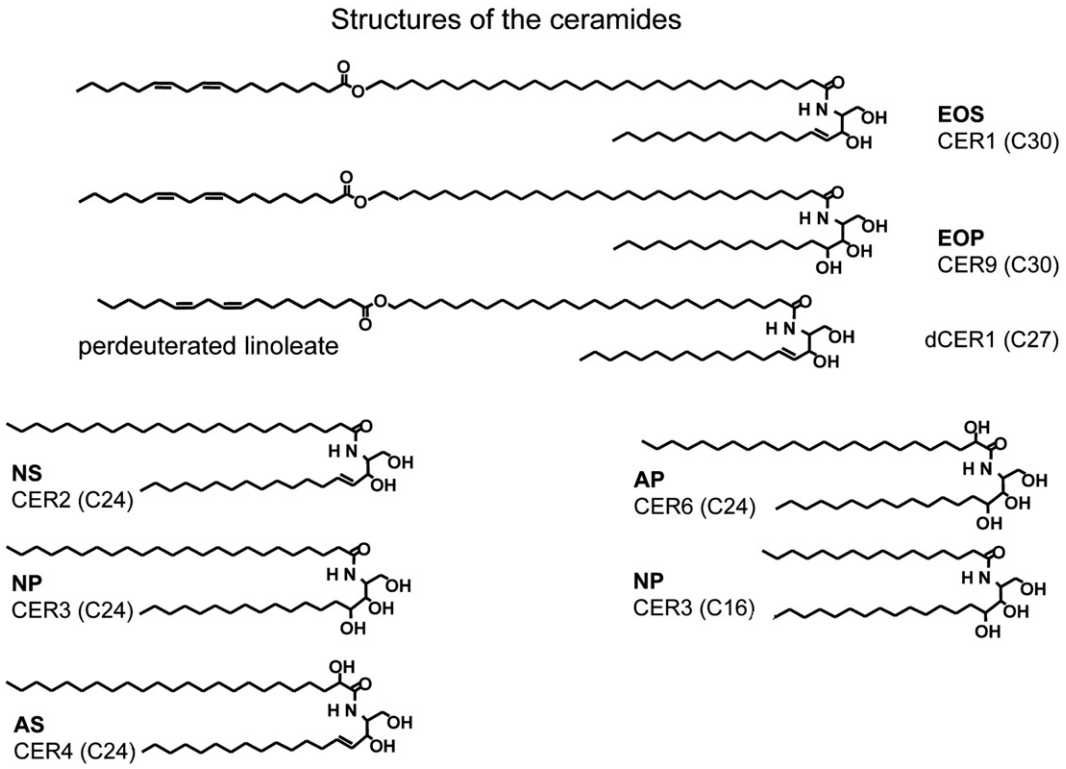

Fig. 1. The structures of the synthetic CERs. In literature two nomenclatures are used to refer to the CER: numbering of the CER and the nomenclature introduced by Motta et al. [22]. In the nomenclature by Motta the name of the CER is dictated by the structure of the CER. P = phytosphingosine base, S = sphingosine base, A = α-hydroxy fatty acid, N = non-hydroxy fatty acid, EO = linoleate linked to an ω-hydroxy fatty acid.

exceptional natural function of the lipid matrix, namely to act as a barrier inhibiting diffusion of compounds.

In recent years we have focused on the phase behavior of mixtures prepared with synthetic CERs with a well-defined fatty acid chain length. The CER subclasses selected for these studies are shown in Fig. 1, and are derived from either sphingosine (CER1, CER2 and CER4) or phytosphingosine (CER3 and CER6). The molecular architecture of CER1 is exceptional in that an unsaturated linoleic acid is chemically bound to a very long ω-hydroxy fatty acid. In a previous study we selected a CER composition mimicking that present in pig SC. This CER composition is presented in Table 1 and is referred to as the synCER mixture. It was demonstrated that this synCER mixture when mixed with CHOL and FFA forms both lamellar phases and laterally packed crystalline domains [13]. This is similar as in CER:CHOL:FFA mixtures prepared from native CERs.

X-ray diffraction provides detailed information about lamellar phases and crystalline lateral packing. FTIR allows the simultaneous investigation of the packing and conformational ordering of the protonated and deuterated lipids and therefore provides information on the mixing properties of different lipid classes in one lattice. It has shown that fatty acids and human CERs participate in a single orthorhombic lattice, while in mixtures with only a single CER and a single FFA often phase separation is encountered [8,23–27].

As the variation in chain length distribution in the synCER mixture is drastically reduced compared to that in native CER mixtures, the question arises whether the synCERs participate in one lattice with the FFAs. Therefore, in the first part of this paper we present FTIR studies using mixtures prepared from synCER, CHOL and FFA. These studies show that synCERs form crystalline mixtures with FFAs and CHOL, similarly as observed for their native counterparts. Furthermore, their thermotropic behavior is also very similar to that observed using mixtures prepared from human CERs. Therefore, the synCER:CHOL:FFA mixtures serve as an excellent tool to examine the role the various lipid subclasses play in the lipid phase behavior and mixing properties. In the present study these mixtures are used i) to examine the role of the linoleate moiety on the formation of fluid domains in the crystalline lattice. This is of interest as the linoleate moiety is the only unsaturated fatty acid chain in the lipid mixture and only little information is available on the coexistence of fluid and crystalline domains in these mixtures and ii) to reduce the number of CER subclasses in the mixtures from 5 to 3. The CER subclasses were selected based on the head group architecture. Mixtures were prepared from only either sphingosine derived CER, phytosphingosine derived CER, or non-hydroxy fatty acid CER. In this way the role of the CER head group architecture on the lateral packing, conformational disordering and mixing

Table 1
The composition of the various synthetic CER mixtures expressed in molar percentages

	CER1 C30*	dCER1 C27*	CER9 C30*	CER2 C24*	CER3 C24*	CER3 C16*	CER4 C24*	CER6 C24*
synCER	15			51	16	9	4	5
synCER DL		15		51	16	9	4	5
sphingoCER	15			78.8			6.2	
phytoCER			15		45.3	25.5		14.2
Non-hydroCER	15			57	17.9	10.1		

* Acyl chain length of the CER Fig. 1.

properties was studied. This is of great importance for understanding the deviation in phase behavior in e.g. SC of diseased skin, in which often a different lipid composition and organization is encountered compared to SC of healthy skin.

2. Materials and methods

The synthetic CERs CER1(C30:0), CER2(C24:0), CER3(C24:0), CER3 (C16:0), CER4(C24:0), CER6(C24:0), CER9(C30:0) and CER1(C27:0) with a deuterated linoleate moiety (referred to as dCER1) were kindly provided by Cosmoferm (Delft, The Netherlands). The perdeuterated FFAs (referred to as DFFAs) with chain lengths of C18:0 and C20:0 were purchased from Cambridge Isotope Laboratories (Andover, Massachusetts). The DFFAs with chain lengths of C16:0 and C22:0 were obtained from Larodan (Malmö, Sweden). DFFAs with a chain length of C24:0 was obtained from Arc Laboratories B.V. (Apeldoorn, The Netherlands). CHOL, FFAs and (deuterated) acetate buffer salts were provided by Sigma-Aldrich Chemie GmbH (Schnelldorf, Germany). All organic solvents used were of analytical grade and manufactured by Labscan Ltd. (Dublin, Ireland). All chemicals used were of analytical grade and all solutions were prepared in Millipore water.

2.1. Preparation of lipid mixtures

The lipid mixtures were prepared by dissolving 1.5 mg of the lipids in 200 µl of chloroform/methanol (2:1, v/v). A Linomat IV (CAMAG, Muttenz, Switzerland) was used to spray the lipid mixtures at a rate of 12 sec/µl under a continuous nitrogen stream over an area of one square centimeter on an AgBr window. The sample applicator was adapted with an extra axis perpendicular to the existing axis allowing application in two directions simultaneously. The samples were equilibrated for 10 min at a temperature of 68 °C. Subsequently, the samples were slowly cooled down to room temperature and hydrated with 25 µl of a deuterated acetate buffer of pH 5.0 (50 mM). Deuterated buffer was used in order to avoid interference with the contours of interest in the FTIR spectrum. To homogenize the sample, 10 freeze-thawing cycles were carried out between −20 °C and room temperature. To equilibrate the samples the time period between the spraying of the samples and the FTIR measurements was between 24 h and 48 h. A longer equilibration period did not change the FTIR spectrum. The composition of the samples selected for the measurements is provided below. All studies were performed using either equimolar CER:CHOL or CER:CHOL:FFA mixtures. The FFA mixture consisted of fatty acids with chain lengths of C16:0, C18:0, C20:0, C22:0 and C24:0 in a molar ratio of 1.8%, 4.0%, 7.6%, 47.8% and 38.9%, respectively, mimicking the composition in SC [5]. With respect to the CER mixture, the following compositions were selected. An overview of the various synthetic CER mixtures used in this study is provided in Table 1.

i) The CER mixture was composed of CER1(C30:0), CER2(C24:0), CER3(C24:0), CER4(C24:0), CER3(C16:0) and CER6(C24:0) with molar percentages of 15%, 51%, 16%, 4%, 9% and 5%, respectively. The CER composition resembles that in pig SC and is referred to as synCER [28].

ii) The role of the linoleate moiety of CER1 in the formation of domains with high conformational disorder was examined by replacing CER1 by CER1 with a deuterated linoleic acid (dCER1). This mixture is referred to as synCER DL, see Fig. 1 and Table 1.

iii) To study the influence of the reduction in CER subclasses on the lipid organization, CER mixtures were selected composed of either only sphingosine derived (sphingoCER), phytosphingosine derived (phytoCER) or non-hydroxy derived CER (non-hydroCER). The molar ratio between the various selected CERs in each mixture was equal to that in the synCER mixture, except for CER1, which was kept constant to 15 mol% of the total CER mixture. Furthermore, as CER1 is sphingosine derived, it was replaced by CER9 (phytosphingosine derived) in the phytoCER mixture, see Fig. 1 and Table 1.

2.2. FTIR measurements

A BIORAD FTS4000 FTIR spectrometer (Cambridge, Massachusetts) equipped with a broad-band mercury cadmium telluride (MCT) detector, cooled with liquid nitrogen was used to acquire spectra. The sample cell was closed by a 2nd AgBr window. The sample was under continuous dry air purge starting 30 min before the data acquisition. The spectra were collected in transmission mode, as a co-addition of 256 scans at 1 cm^{-1} resolution during 4 min. The lipid phase behavior was examined between 20 °C and 100 °C by increasing the sample temperature at a heating rate of 0.25 °C/min. Bio-Rad Win-IR Pro 3.0 software from Biorad (Cambridge, Massachusetts) was used. Most of the mixtures were measured at least twice. The results were very reproducible.

2.3. Small angle X-ray diffraction

All measurements were performed at the European Synchrotron Radiation Facility (ESRF, Grenoble) using station BM26B. A more detailed description of this beamline has been given elsewhere [29]. The X-ray wavelength and the sample-to-detector distance were 1.24 Å and 1.7 m, respectively. Diffraction data were collected on a two-dimensional multiwire gas-filled area detector. The spatial calibration of this detector was performed using silver behenate. The samples were mounted in a specially designed sample holder with mica windows. All measurements were recorded at room temperature for a period of 10 min.

The dimensionless scattering intensity (I) was measured as a function of the scattering vector q (in reciprocal nm). The latter is defined as $q=(4\pi\sin\theta)/\lambda$, in which θ is the scattering angle and λ is the wavelength. From the positions of a series of equidistant peaks (q_n), the periodicity, or d-spacing, of a lamellar phase was calculated using the equation $q_n=2n\pi/d$, n being the order number of the diffraction peak. All mixtures were measured at least twice.

3. Results

In the FTIR spectra of the lipid mixtures we focus on several vibrational modes providing information on the ordering and lateral packing of the hydrocarbon chains. The symmetric CH_2 and CD_2 stretching modes provide information about the conformational order–disorder transitions. In the spectrum these vibrations are ranged between 2846 and 2855 cm^{-1} (CH_2 symmetric stretching mode) and 2086–2098 cm^{-1} (CD_2 symmetric stretching mode). Information on the packing of the carbon chains perpendicular to the chain direction is obtained from the CH_2 and CD_2 scissoring modes (located at 1462–1473 cm^{-1} and 1085–1095 cm^{-1}, respectively). When the chains are hexagonally packed, a singlet corresponding to the CH_2 scissoring band is observed at around 1468 cm^{-1}, while in a crystalline orthorhombic lattice a broadening or splitting of the contours occurs due to interactions of adjacent chains via a short-range coupling. The width of the splitting is an indication for the domain size of the orthorhombic lattice [30]. However, when deuterated and protonated chains participate in one lattice, the scissoring modes will not interact and the vibrational coupling will not occur. Consequently, the splitting of the peak in the scissoring region of the spectrum will disappear. Therefore, in an orthorhombic lattice, elimination of the coupling after replacing protonated lipids by deuterated ones is indicative for participation of deuterated and protonated lipid classes in one lattice.

3.1. Mixtures prepared with synCERs

As CERs, CHOL and FFAs are the main lipid classes in SC, these lipids were selected for the FTIR measurements. First the results of the synCER mixture without additional lipid classes will be presented. Subsequently the results of the equimolar synCER:CHOL and synCER:CHOL:FFA mixtures will be described. In order to determine whether synCERs and FFAs participate in one lattice, protonated FFAs are replaced by their deuterated counterparts in some lipid mixtures.

Fig. 2a shows the thermotropic changes of the symmetric CH_2 stretching frequency of the synCER mixture between 20 °C and 100 °C. At 20 °C, the symmetric CH_2 frequency is located at 2846 cm^{-1}. A gradual change in frequency is observed during a temperature rise from 20 to 66 °C. Between 66 °C and 90 °C a strong frequency shift from 2847.0 cm^{-1} to 2852.9 cm^{-1} occurs. This is indicative for an ordered to a disordered lipid phase transition. Fig. 2a also shows the thermotropic response of the CH_2 stretching mode of the equimolar synCER:CHOL mixture. At 20 °C the CH_2 symmetric stretching modes are located at 2846.9 cm^{-1}. An increase in temperature to 64 °C increases the frequency only slightly. As a result of a rise in temperature from 64 °C to 90 °C, the symmetric CH_2 stretching mode gradually shifts from 2848.3 cm^{-1} to 2853 cm^{-1}. Fig. 2b depicts the CH_2 scissoring modes for the synCER and synCER:CHOL mixtures at 20 °C. The CH_2 scissoring frequency is a singlet and is located at 1467.4 cm^{-1} for both mixtures. This has been confirmed by the CH_2 rocking mode: only a singlet is observed at 720 cm^{-1} (not shown). The absence of splitting in the synCER and synCER:CHOL mixture is indicative for the absence of an orthorhombic phase.

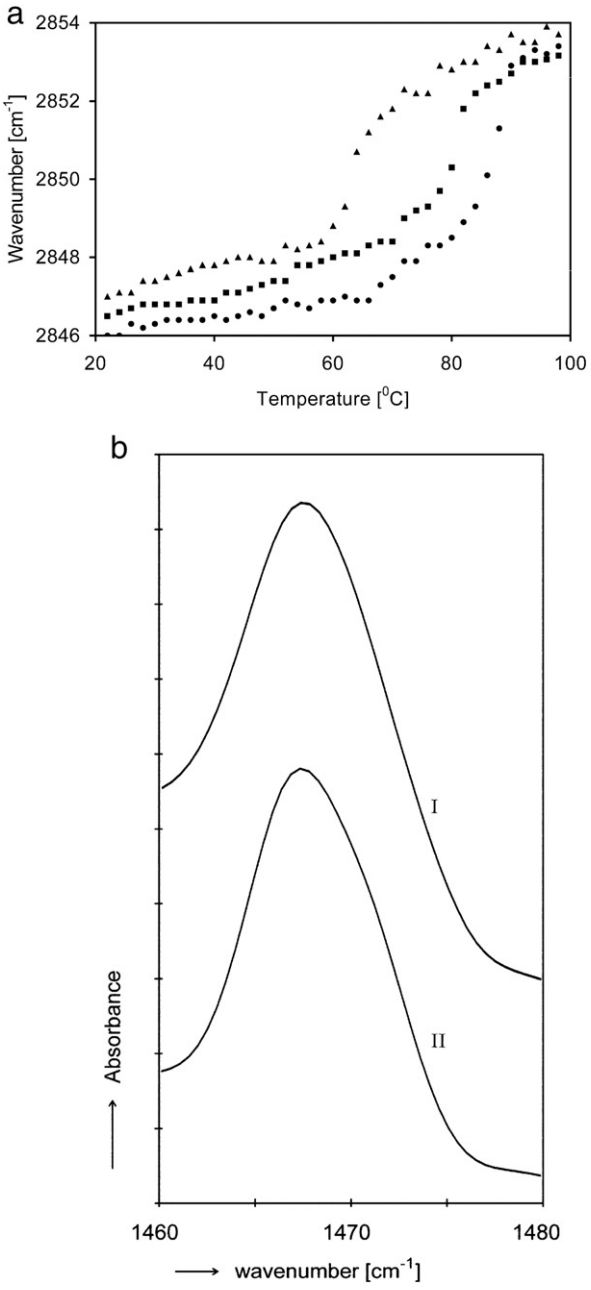

Fig. 2. FTIR spectra and thermotropic response of the synCER, synCER:CHOL and synCER:CHOL:FFA mixtures. (a) The thermotropic response of the symmetric CH_2 frequency modes of synCER (●), equimolar synCER:CHOL mixtures (■) and equimolar synCER:CHOL:FFA mixtures (▲). (b) The original spectra of the CH_2 scissoring modes of the synCER and synCER:CHOL mixture at 20 °C.

In order to investigate the role of FFAs in the lipid organization, the equimolar synCER:CHOL:FFA mixture was also examined. As depicted in Fig. 2a, the symmetric stretching frequency at room temperature is located at 2847.0 cm^{-1}. At around 30 °C a slight frequency increase occurs from 2847.0 to 2847.6 cm^{-1}, which may indicate an orthorhombic-hexagonal phase transition in this temperature range. This transition, however, is much more obvious from the scissoring vibrations as shown below. A further increase in temperature results in a gradual increase in the frequency to 2848.9 cm^{-1} at 60 °C. A temperature rise above 60 °C results in a clear shift in the symmetric CH_2 stretching frequency to 2853.5 cm^{-1} at 88 °C. This shift represents a conformational order–disorder phase transition. The midpoint of the transition is around 64 °C, which is lower as observed in the synCER (86 °C) and synCER:CHOL (80 °C) mixtures. With respect to the CH_2 scissoring contours, a clear splitting with peak positions at 1463 cm^{-1} and 1473.3 cm^{-1} at 20 °C is observed, see Fig. 3a. This demonstrates the presence of an orthorhombic lattice. Large domains with orthorhombic organization (domains larger than 100 lipids) are formed as the magnitude of the CH_2 splitting almost approaches the maximum value of 11 cm^{-1} [30]. In between the doublet band a weak singlet is observed at a position of around 1467 cm^{-1} indicating that a subpopulation of lipids is forming a hexagonal or liquid packing. The weak singlet can also partly be caused by CHOL, as the spectrum of CHOL shows a peak in this region. An increase in temperature results in a weakening of the doublet and an increase in intensity of the singlet. The band at 1463 cm^{-1} disappears at 32 °C, while the peak at ~1473 cm^{-1} is observed until 36 °C, representing a coexistence of an orthorhombic and hexagonal packing between 20 °C and 36 °C. However, at temperatures above 36 °C only a singlet at 1466.8 cm^{-1} is detected, demonstrating that lipids in the synCER:CHOL:FFA mixture participate in the ordered hexagonal packing. The contour of the rocking vibrations displays also a splitting at band positions of 719.4 cm^{-1} and 730 cm^{-1} (not shown) confirming that the lipids participate in an orthorhombic lattice. This splitting disappears above 36 °C, similarly as observed for the scissoring mode.

In order to determine whether FFAs and synCERs participate in a single lattice, equimolar mixtures of synCER:CHOL:DFFA were also examined. As the presence of FFAs is the determining factor in the formation of the orthorhombic lattice, we focused on the reduction in splitting of the scissoring mode when replacing FFAs by DFFAs. Fig. 3b shows the CD_2 scissoring modes of the synCER:CHOL:DFFA mixture. Only a weak splitting is observed until 30 °C, located at 1086.3 cm^{-1} and 1090.3 cm^{-1}. No doublet is observed above a temperature of 30 °C, indicating that at skin temperature no separate domains of DFFAs are present in an orthorhombic lattice. The CH_2 rocking modes of the synCER:CHOL:DFFA mixture are plotted in Fig. 3c. Very surprisingly, a doublet is observed that turns into a singlet at around 30 °C. This strongly suggests that synCERs and CHOL form domains with orthorhombic packing in the presence of DFFAs. The formation of small domains with orthorhombic packing is confirmed by the contours of the scissoring vibrations (not shown).

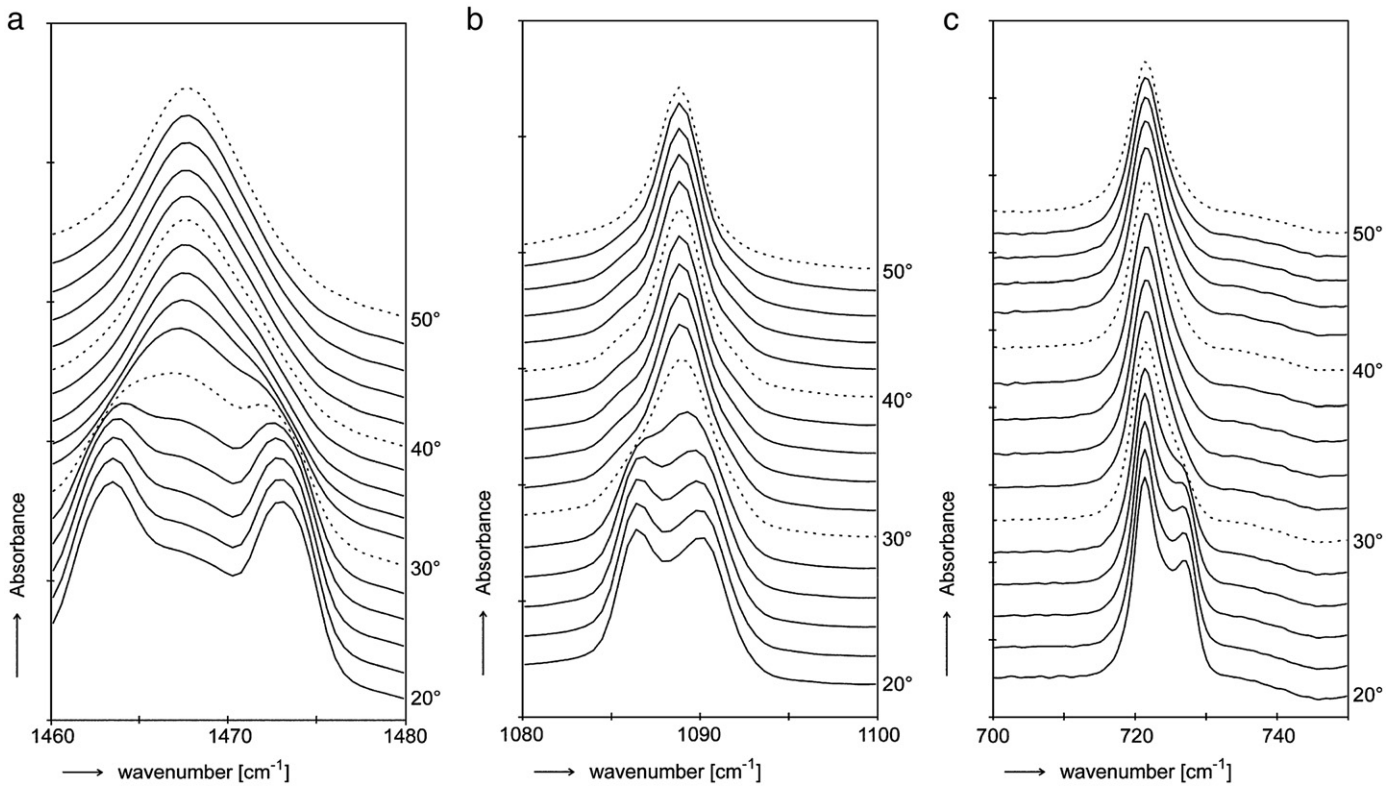

Fig. 3. FTIR spectra of synCER:CHOL:FFA and synCER:CHOL:DFFA mixtures. (a) The original spectra of the CH_2 scissoring modes of the equimolar synCER:CHOL:FFA mixture measured as function of temperature. (b) The original spectra of the CD_2 scissoring modes of the equimolar synCER:CHOL:DFFA mixture measured as function of temperature. (c) The original spectra of the CH_2 rocking modes of the equimolar synCER:CHOL:DFFA mixture measured as function of temperature.

3.2. The role of CER1 in the formation of disordered domains

As CER1 contains a linoleic acid linked to a very long ω-hydroxy fatty acid, the question arises whether domains with conformational disordering are present in the lipid mixture at room temperature and, even more important, at skin temperature of around 32 °C. In order to examine the conformational ordering, CER1 was replaced by CER1 with a perdeuterated linoleate (dCER1) in the synCER mixtures. In this mixture only a small population of the lipids is deuterated. Therefore, first studies were performed with equimolar synCER:CHOL:FFA mixtures. In these mixtures a small population of FFAs was replaced by DFFAs resulting in the same level of CD_2 units present as in the dCER1 containing mixtures. These mixtures are referred to as synCER:CHOL:FFA-DFFA. In Fig. 4 the thermotropic CD_2 symmetric stretching frequencies of the equimolar synCER:CHOL:FFA-DFFA are plotted. At 20 °C the CD_2 symmetric stretching contour is located at a position of 2089.4 cm^{-1}, indicating a conformational ordering. A gradual increase in temperature does not change the peak position until a temperature of 60 °C is reached. Above this temperature the frequency of the stretching mode shifts to 2096.6 cm^{-1} at 68 °C. In addition, a broadening of the scissoring band is observed (not shown). Both observations demonstrate an order–disorder phase transition in a similar temperature range as for the CH_2 stretching modes depicted in Fig. 2a.

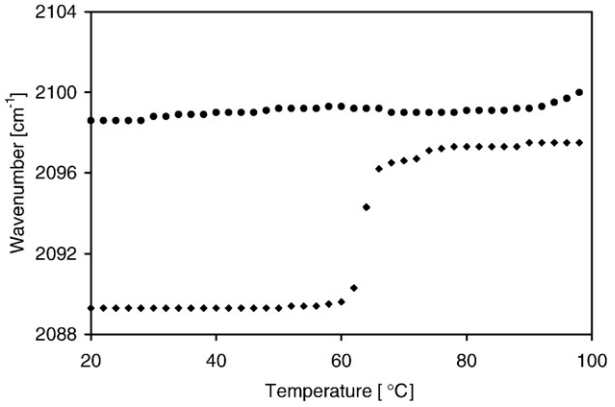

Fig. 4. The thermotropic responses of the frequencies of the symmetric CD_2 stretching modes of the equimolar synCER:CHOL:FFA-DFFA mixture (referred to as I) and of the equimolar synCER DL:CHOL:FFA mixture (referred to as II).

In subsequent studies the CD_2 symmetric stretching frequencies of the equimolar synCER DL:CHOL:FFA mixtures were examined between 20 °C and 90 °C. In Fig. 4 the corresponding thermotropic responses are provided between 20 °C and 90 °C. At 20 °C the CD_2 symmetric stretching mode is located near 2099 cm^{-1} and the contours are very broad (not shown). Furthermore, the position of contours does not change upon increasing the temperature until a temperature of 90 °C is reached. This provides clear evidence for a conformational disorder of the linoleate moiety at room and skin temperature.

3.3. The influence of the CER head group architecture on the lipid organization

Not only the lipid chain length, but also the reduction in the number of CERs and the CER head group architecture may effect the conformational ordering and packing of the hydrocarbon chains in the CER:CHOL:FFA mixtures. In order to study the role of CER head group architecture, mixtures with either sphingoCER, phytoCER or non-hydroCER were examined. As no information is available about the lamellar organization in these mixtures, X-ray diffraction profiles of the equimolar mixtures were measured at room temperature. The diffraction patterns are provided in Fig. 5. The small angle X-ray

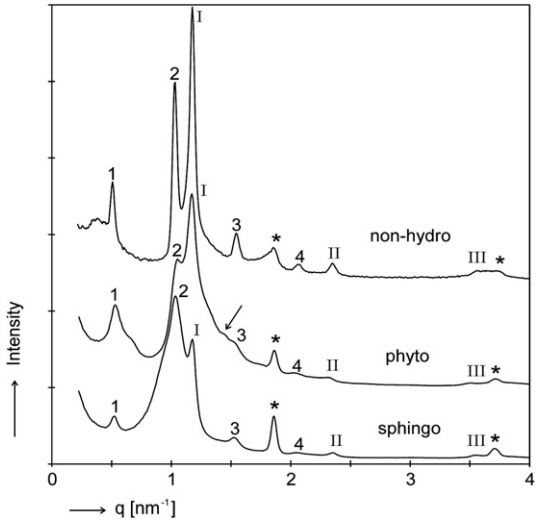

Fig. 5. X-ray diffraction curves of mixtures prepared from equimolar sphingoCER:CHOL: FFA, phytoCER:CHOL:FFA and non-hydroCER:CHOL:FFA mixtures. The diffraction patterns are plotted as a function of the scattering vector q. The LPP is identified by 4 diffraction orders: 1st, 2nd, 3rd and 4th order located at 0.52, 1.03, 1.54 and 2.06 cm^{-1}. The SPP is identified by three orders referred to as I, II and III in the figure. These are located at 1.18, 2.35 and 3.53 nm^{-1}.* identifies the diffraction peaks (3.36 nm and 1.87 nm) spacings of crystalline CHOL located at 1.86 and 3.74 nm^{-1}.

diffraction pattern of the equimolar sphingoCER:CHOL:FFA mixture is plotted in the curve indicated by sphingo. Four orders of diffraction peaks that attribute to a lamellar phase with a repeat distance of 12.2 nm are visible. In addition, 3 peaks are present which are attributed to the SPP with a repeat distance of 5.4 nm. This demonstrates that the lamellar phases that are also present in human SC are formed in this mixture. Besides the formation of the lamellar phases, CHOL phase separates in crystalline domains. Fig. 5 also provides the diffraction pattern of the equimolar phytoCER:CHOL: FFA mixture. This diffraction pattern reveals the 4 orders of the LPP with a repeat distance of 12.2 nm, but on the right-hand side of the 1st order a weak shoulder is present attributed to phase separated CER9. This is accompanied with a weak shoulder on the right-hand side of the 1st order of the SPP, which is most probably the 2nd order of that phase (see arrow). In addition the 2nd and 3rd order diffraction peaks of the SPP are also identified. The diffraction pattern of the equimolar non-hydroCER:CHOL:FFA mixture is also provided in Fig. 5. At least 4 orders of sharp diffraction peaks (1st, 2nd, 3rd and 4th order) are attributed to the LPP with a repeat distance of 12.2 nm. In addition, three diffraction peaks can be attributed to the SPP with a repeat distance of 5.4 nm. A small amount of CHOL phase separates as indicated by the 3.38 nm and 1.67 nm reflections. These studies clearly demonstrate that mixtures prepared with either phytosphingosine based, sphingosine based or non-hydroxy based synthetic CERs are able to form the LPP.

Fig. 6 shows the thermotropic response of the CH_2 symmetric stretching mode frequencies of the equimolar CER:CHOL:FFA mixture with either sphingoCER, phytoCER or non-hydroCER as the CER mixture. At 20 °C, the CH_2 symmetric stretching frequencies of the different mixtures indicate conformational ordering, since all the frequencies are below 2850 cm^{-1}. The mixture containing phytoCER has the lowest initial stretching frequency (2845 cm^{-1}), indicating the highest conformational ordering of the lipids. When increasing the temperature and focusing first on the sphingoCER mixtures, a slight increase in frequency is observed between 32 °C and 46 °C (from 2849.5 cm^{-1} to 2850.1 cm^{-1}), which may indicate the transition of an orthorhombic to a hexagonal packing. Further increase in temperature results in a frequency shift from 2850.1 cm^{-1} to 2853.7 cm^{-1} between 60 °C and 82 °C. As far as the phytoCER and non-hydroCER containing mixtures are concerned, no frequency shifts were observed between 30 °C and 40 °C. The order–disorder transition is observed from 2848.4 cm^{-1} to 2853.7 cm^{-1} between 58 °C and 88 °C for the mixtures containing the non-hydroCER. This conformational disordering transition is also observed in the mixture containing the phytoCER based mixture, but the transition occurs in a temperature range approximately 10 degrees higher, namely between 70 °C and 88 °C (from 2846.0 cm^{-1} to 2853.7 cm^{-1}). Fig. 7a shows the CH_2 scissoring modes of the equimolar phytoCER:CHOL:FFA, sphingoCER:CHOL:FFA, and non-hydroCER:CHOL:FFA mixture at 20 °C. In the spectrum of the sphingoCER:CHOL:FFA mixture, a doublet contour is observed with components at 1463 cm^{-1} and 1473.4 cm^{-1}, characteristic for the formation of domains with orthorhombic packing. A weak singlet is observed at a position around 1467 cm^{-1}, indicative for a subfraction of lipids forming either a hexagonal or a liquid phase. The FTIR spectrum of the phytoCER:CHOL:FFA mixture shows a weaker doublet at 1463.4 cm^{-1} and 1472.6 cm^{-1} and a stronger singlet at 1466.9 cm^{-1} at 20 °C, clearly demonstrating a hexagonal packing already at 20 °C. The magnitude of splitting (9.2 cm^{-1}) indicates the formation of large domains with orthorhombic organization. The CH_2 scissoring modes of the non-hydroCER:CHOL:FFA mixture are similar to those in the spectra of the sphingoCER based mixture with a doublet and a weak singlet around 1467 cm^{-1} in the spectrum at 20°C.

The thermotropic responses of the CH_2 scissoring frequencies of the three mixtures are plotted in Fig. 7b–d. When increasing the temperature of the sphingoCER:CHOL:FFA mixture, a reduction in intensity of the doublet starts at around 30 °C, while the singlet increases in intensity demonstrating the orthorhombic to hexagonal phase transition (not shown). The low frequency component disappears at around 36 °C, while the high frequency component collapses at around 58 °C, suggesting the completion of the transition to a fluid or a hexagonal packing. With respect to the phytoCER:CHOL: FFA mixture, no thermotropic response in the scissoring contours are observed until 52 °C. Then the frequencies shift and the doublet disappears at around 58 °C. The results are confirmed by CH_2 rocking modes showing a splitting until 58 °C at 720.9 cm^{-1} and 728.3 cm^{-1} (not shown). Also in the non-hydroCER:CHOL:FFA mixture the doublet disappears at around 58 °C, indicating the coexistence of an orthorhombic and a hexagonal phase in a wide temperature range. The CH_2 rocking modes in the spectrum confirm these results (not shown).

The data presented above show that at elevated temperatures a small population of lipids forms the orthorhombic packing in the equimolar mixtures based on phytoCER, sphingoCER or nonhydroCER mixtures. As the FFA mixture forms an orthorhombic phase until a temperature of 60 °C is reached in the absence of CHOL and CERs [8], the question remains whether the doublet in the spectrum of the equimolar CER:CHOL:FFA mixtures is a result of phase-separated FFAs

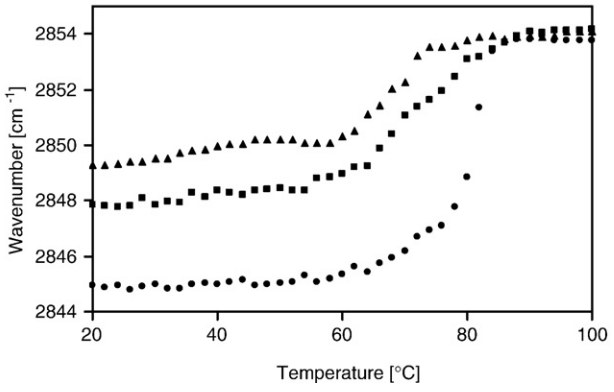

Fig. 6. The thermotropic response of the symmetric CH_2 stretching frequency modes of sphingoCER:CHOL:FFA (▲), equimolar phytoCER:CHOL:FFA mixtures (●) and equimolar non-hydroCER:CHOL:FFA mixtures (■).

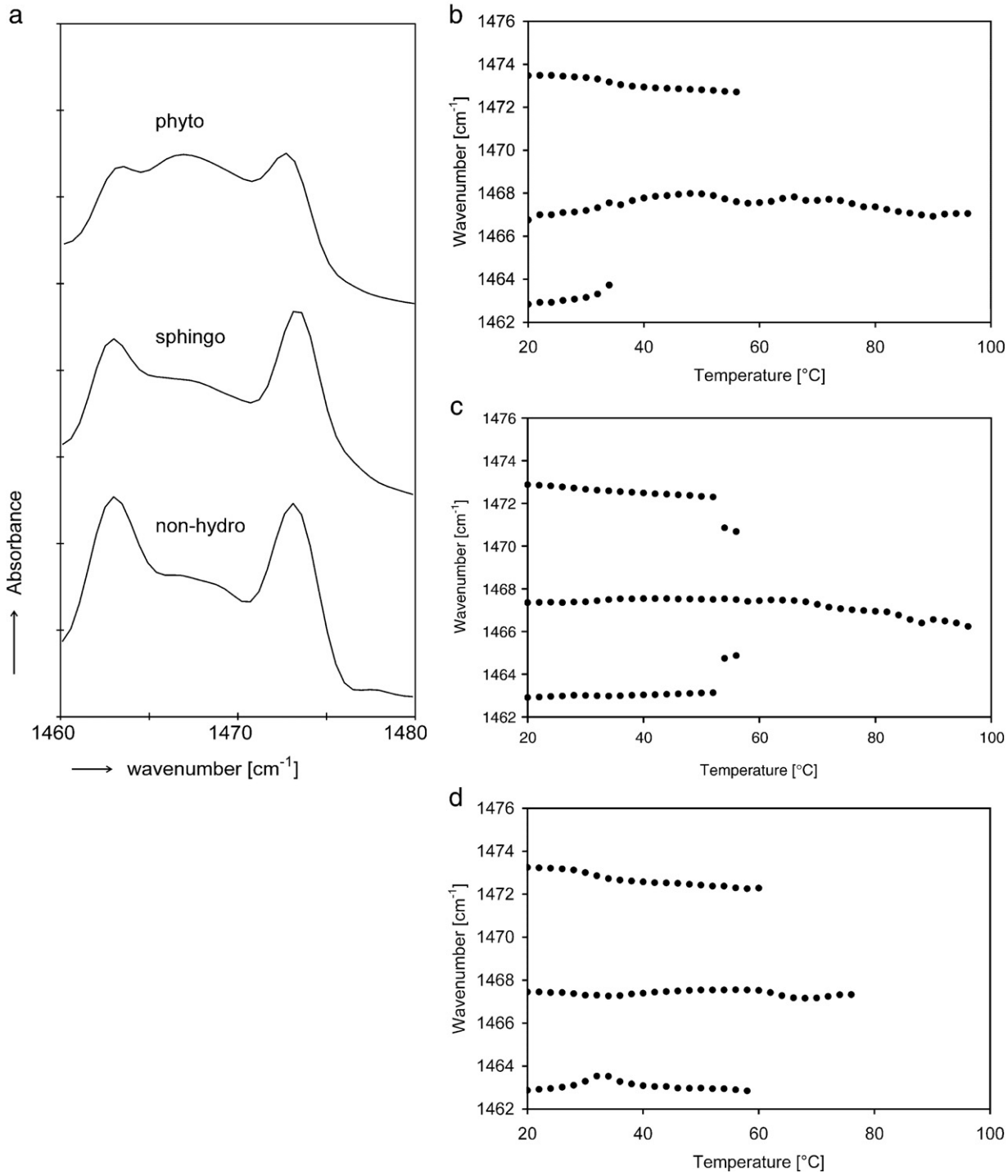

Fig. 7. FTIR spectrum and thermotropic responses of mixtures consisting of CERs varying in head group architecture. (a) The CH_2 scissoring mode of the equimolar sphingoCER:CHOL:FFA, phytoCER:CHOL:FFA and non-hydroCER:CHOL:FFA mixtures at 20 °C. (b) The thermotropic responses of the CH_2 scissoring modes of the equimolar sphingoCER:CHOL:FFA mixtures. (c) The thermotropic responses of the CH_2 scissoring modes of the equimolar phytoCER:CHOL:FFA mixtures. (d) The thermotropic responses of the CH_2 scissoring modes of the equimolar non-hydroCER:CHOL:FFA mixtures.

or due to the formation of an orthorhombic packing in which CERs and FFAs participate. In order to answer this question, FFAs were replaced by DFFAs and FTIR spectra were collected.

Fig. 8a shows the CD_2 scissoring contours of the sphingoCER:CHOL:DFFA mixture at 20 °C and 40 °C. A splitting of the contour with frequencies at 1086.4 cm^{-1} and 1090.8 cm^{-1} is observed between 20 °C and 30 °C. Between 30 °C and 40 °C the doublet gradually disappears and a singlet at a position of 1089.3 cm^{-1} is formed with weak shoulders on both sides of this singlet. These shoulders disappear at 50 °C (not shown). The CD_2 scissoring contours in the spectrum of the non-hydroCER:CHOL:DFFA mixture at 20 °C and 40 °C are also presented in Fig. 8a. A shoulder is observed in the low frequency region of the contour at around 1087 cm^{-1} indicating the presence of domains with orthorhombic organization formed by DFFAs. However, this shoulder disappears at 30 °C.

When focusing on the CH_2 rocking contours of the sphingoCER:CHOL:DFFA mixture (Fig. 8b), a weak doublet is observed with frequencies at positions of 722 and 727.5 cm^{-1}. The presence of a

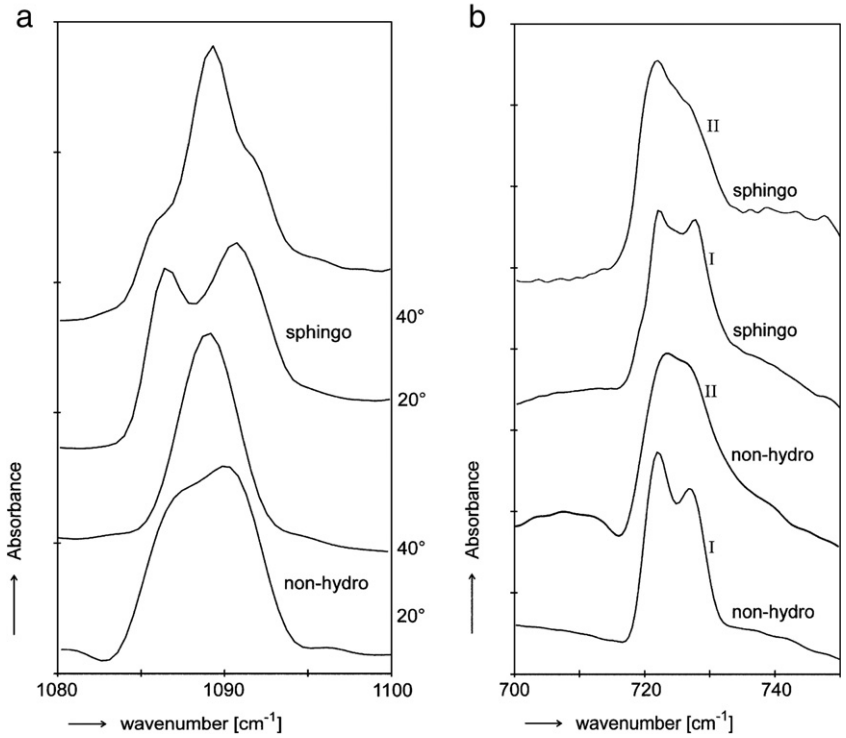

Fig. 8. FTIR spectra of mixtures consisting of CERs varying in head group architecture. (a) The CD_2 scissoring mode of the equimolar sphingoCER:CHOL:DFFA and non-hydroCER:CHOL:DFFA mixtures at 20 °C and 40 °C. (b) The CH_2 rocking mode at 20 °C of the equimolar sphingoCER:CHOL:DFFA mixture (I), sphingoCER mixtures (II), equimolar non-hydroCER:CHOL:DFFA mixture (I) and non-hydroCER mixture(II).

doublet for the CH_2 rocking contours has also been observed in the synCER:CHOL:DFFA mixtures, see Fig. 3c. When comparing to the sphingoCER mixtures in the absence of CHOL and FFAs, a weaker doublet is observed at frequencies of 722 cm^{-1} and 729 cm^{-1} at 20 °C (Fig. 8b). The CH_2 rocking contours of the non-hydroCER:CHOL:DFFA mixture are also depicted in Fig. 8b. A doublet is observed with frequency positions at 721 cm^{-1} and 728 cm^{-1} indicating CH_2 regions with an orthorhombic packing. This splitting disappears at around 30 °C (not shown). When examining the non-hydroCER mixture in the absence of FFAs and CHOL (Fig. 8b) at 20 °C, the CH_2 rocking modes show a peak located at 721 cm^{-1} with a weak shoulder located at approximately 727 cm^{-1}. As far as the phytoCERCHOL:DFFA mixture is concerned, the CD_2 and CH_2 scissoring and rocking contours reveal only a slight broadening. This broadening disappears at around 30 °C (not shown).

4. Discussion

In a recent study the phase behavior and conformational ordering of mixtures prepared with native human CERs (hCERs) were reported [8]. One of the most important conclusions drawn from that study was the participation of FFAs and hCERs in one lattice. This contrasts the results obtained with mixtures prepared from one single synthetic CER and a single FFA [24,31–33]. In the present study, the main focus was to elucidate the conformational ordering and lateral packing of lipid mixtures prepared with the synCER mixture. This is of interest as in the synCER mixture the variation in fatty acid chain length and head group architecture is less abundant than in isolated hCERs. A wide variation in acyl chain lengths has been reported in the latter: hCER acyl chain length varies between 12 and 34 carbon atoms. The differences in distribution may affect the mixing properties of the various lipid classes. Therefore, we will first discuss mixtures prepared with synCER in comparison to hCERs containing mixtures [8].

4.1. A comparison between mixtures based on either hCER or synCER

Previous X-ray diffraction studies revealed that the lamellar organization of mixtures prepared with synCERs are very similar to that of mixtures prepared with hCERs: the lipids form the crystalline LPP and SPP, resembling the lipid organization in SC [34,35]. When comparing the lateral packing and conformational disordering at 20 °C and 32 °C (skin temperature) as determined by FTIR, hCER:CHOL and synCER:CHOL mixtures form a hexagonal lattice. Addition of FFAs to synCER:CHOL:FFA and to hCER:CHOL:FFA mixtures promotes the formation of an orthorhombic sublattice [8]. However, a clear difference is observed when comparing the thermotropic response of the CH_2 symmetric stretching modes. In synCER and synCER:CHOL mixtures the order–disorder transition occurs at temperatures much higher than observed for the synCER:CHOL:FFA, hCER:CHOL and hCER:CHOL:FFA mixtures [8]. The higher transition temperatures of synCER and synCER:CHOL mixtures might be due to the more homogenous acyl chain length distribution of the synCER mixture compared to that in the hCER mixture.

The mixing properties of FFAs and synCERs in the orthorhombic lattice of the equimolar synCER:CHOL:DFFA were also examined. The degree of mixing of synCERs and FFAs can only be obtained from the CD_2 scissoring modes, as domains with synCERs and CHOL form mainly a hexagonal lateral packing. In a previous study it was reported that the pure DFFA mixture forms an orthorhombic lateral packing with peak positions at 1085.4 and 1092.6 cm^{-1} which is observed until 68 °C [8]. In our present study, the peak intensities of the doublet are drastically reduced (Fig. 3b) compared to the pure DFFA. This finding strongly suggests that a large population of DFFAs and synthetic CERs participate in one lattice. Only a small fraction of DFFAs phase separates in domains with orthorhombic organization or is present in the same lattice, but at a slightly higher DFFA concentration as observed by Snyder et al. [36] for C36H/C36D mixtures. Furthermore, the magnitude of splitting reduces from 7.2 cm^{-1} (DFFA mixture only) to 4.0 cm^{-1} suggesting small sizes of DFFA rich domains. A similar

splitting was also observed for the hCER:CHOL:DFFA mixtures [8]. Furthermore, the splitting disappears already at 30 °C, which is at a much lower temperature than 68 °C in the spectrum of the pure DFFA mixture. This was also observed for the CD_2 scissoring mode in the hCER:CHOL:DFFA mixtures. This may indicate that the splitting is indeed due to higher local concentrations of DFFA in the same lattice as the synCERs and that it is not due to pure DFFA domains.

When focusing on the CH_2 rocking mode in the synCER:CHOL:DFFA mixtures (Fig. 3c), an interesting phenomenon is observed. The CH_2 rocking contours exhibit a doublet. This indicates that besides participation of DFFA and synCER in one lattice and the existence of DFFA rich domains, an orthorhombic lattice is formed by a small fraction of protonated lipids. This is very remarkable as the equimolar synCER:CHOL mixture (absence of FFA) is forming a hexagonal lattice. This indicates the formation of an orthorhombic packing in protonated lipid domains induced by DFFA. There are at least two possible explanations. i) the ability of synCERs to participate in DFFA rich domains is not equal for the various synthetic CER subclasses, resulting in a change in synthetic CER composition in the protonated CER:CHOL rich domains. As discussed below, a change in CER head group architecture may affect the lateral packing or ii) the repeat distance of the LPP is approximately 12–13 nm, indicating that the repeating unit consists of more than one lipid layer. FFAs present in one lipid layer may interact with protonated rich domains by head group interactions, thereby inducing an orthorhombic lateral packing in synCER:CHOL domains. This is possible as the head group interfacial area of the fatty acids (around 0.2 nm^2) is quite small compared to that of CHOL and CER (0.38 nm^2 and 0.40 nm^2, respectively). This reduces the mean interfacial area of head groups in the mixture resulting in a higher packing density of the hydrocarbon chains [37–39]. The presence of protonated lipid rich domains forming an orthorhombic lattice has not been observed in the hCER:CHOL:DFFA mixtures [8]. This difference in behavior may be caused by reduced variation in chain length distribution and head group architecture in the synCER mixture compared to the hCER mixture.

When comparing our results to the in vivo situation in SC with a skin temperature of approximately 32 °C, it is expected that in vivo only very low levels of FFAs form separate domains with an orthorhombic packing. This might be important for maintaining a proper skin barrier function as the existence of separate domains may facilitate the penetration of substances.

In almost all aspects the mixtures containing synCER very closely resemble the properties of hCER containing mixtures and the characteristic properties for the mixtures might even reflect the situation in SC. Therefore, in the second part of our studies the synCER mixture was used to examine two additional aspects, namely i) the role of the linoleate of CER1 in the formation of the fluid domains and ii) the role of the CER head group architecture on the lateral packing, conformational disordering and mixing properties.

4.2. The conformational ordering of the linoleate in the lipid mixtures

Several papers report on the important role of CER1 in the lipid organization of CER containing lipid mixtures in vitro and human SC in vivo [40–44]. These studies demonstrate that CER1 i) plays a prominent role in the formation of the LPP and ii) is important for the skin barrier function [45]. Furthermore, it has been reported that replacement of the linoleate chain in CER1 by a stearate chain also prevents the formation of the LPP and reduces the formation of a fluid phase [42]. However, currently there is no direct evidence that the linoleate moiety is forming a fluid phase. Therefore, in the present study, FTIR measurements were performed with synCER:CHOL:FFA mixtures, in which the protonated linoleate was replaced by its deuterated counterpart (Fig. 1). This permits selectively monitoring of the conformational ordering of the linoleate moiety. No further changes were induced by changing the linoleate by its deuterated counterpart: the CH_2 vibrations (stretching, scissoring and rocking) were similar to those of the mixture in which the linoleate was protonated. As depicted in Fig. 4, the conformational disorder of the linoleate moiety of CER1 is substantially increased compared to the deuterated FFA in the synCER:CHOL:FFA-DFFA mixture. This demonstrates that the linoleate is partitioning in a disordered phase already at 20 °C. The frequency of CD_2 symmetric stretching mode is even higher than observed for the fluid DFFA, which might be due to its linkage to the ω-hydroxy acyl chain of CER1 and, therefore, the absence of a head group chemically linked to the linoleate. However, very peculiar, although the linoleate moiety has a high conformational disorder, translational motion is not permitted as it is fixed by the ω-hydroxy acyl chain of the CER1, which is present in a crystalline packing. Therefore, the linoleate does not preserve all the properties of a fluid phase. We refer to this as a "pseudo fluid" phase. As this is a very interesting phenomenon, in additional studies we replaced hCER1 in the hCER mixture by dCER1 and again examined the conformation disorder of deuterated linoleate chain between 20 °C and 90 °C in the equimolar hCER:CHOL:FFA mixture (not shown). The observed conformational disordering of the deuterated linoleate was very similar to that observed in the synCER DL:CHOL:FFA mixtures: the CD_2 symmetric stretching frequency is located near 2099 cm^{-1} and the contours are very broad, demonstrating that also in these mixtures a pseudo-fluid phase coexists with crystalline domains. Therefore, in these aspects the synCER:CHOL:FFA mixture also resembles closely that of the hCER:CHOL:FFA mixture. The presence of a pseudo fluid phase is in agreement with the sandwich model [11], and also with the mosaic domain model [46]. However, it is not in agreement with the gel-phase model [47].

4.3. The head group architecture of the synthetic CERs affects the lipid organization

As mixtures prepared with synCERs or hCERs behave very similar, we used the synCER mixture as a tool to examine a further reduction in CER subclasses on the lateral packing, conformational disordering and mixing properties. Three synthetic CER mixtures were selected, namely sphingoCERs, phytoCERs and non-hydroCERs. In these mixtures the number of CER subclasses was reduced from 5 to 3. The first question that arises is: is it possible to form the LPP with a reduced variation in head group architecture in equimolar CER:CHOL:FFA mixtures prepared with either sphingoCER, phytoCER or non-hydroCER? X-ray diffraction studies reveal that the three CER:CHOL:FFA mixtures (Fig. 5) form the LPP. The diffraction patterns of mixtures prepared with sphingoCER or phytoCER show a large width at half maximum of the diffraction peaks attributed to the LPP. Furthermore, several peaks in the diffraction curves demonstrate the formation of additional phases. This suggests a reduced ordering of the lipid lamellae and a reduced formation of the LPP compared to equimolar synCER:CHOL:FFA mixtures. This is most clearly encountered in the diffraction curve of the phytoCER:CHOL:FFA mixture. Therefore, reducing the variation in head group architecture reduces the ability of lipid mixtures to form the LPP in a reproducible manner.

When focusing on the conformational ordering of the lipids, the CH_2 symmetric stretching frequency (2845 cm^{-1}) of the phytoCER:CHOL:FFA mixture at 20 °C is very low (Fig. 6). This is remarkable since the hexagonal lattice is dominantly present in this mixture (see below). The spectra of the equimolar mixtures with sphingoCER or non-hydroCER show higher initial CH_2 stretching frequencies despite the presence of an orthorhombic phase at 20 °C. When focusing on the order–disorder transition temperature range, differences are also encountered between the three mixtures. In the phytoCER containing mixtures, the order–disorder transition occurs at a higher temperature compared to the mixtures containing sphingoCER or non-hydroCER. This finding is in agreement with the studies by Rerek et al. [23]. For the pure phytosphingosine derivatives they observed an

order–disorder transition of 15–20 °C higher compared to the pure sphingosine derivatives. They suggested that this difference in transition temperature is caused by enhanced hydrogen bonding interactions between the head groups of the phytosphingosine derivatives, while a smaller head group (sphingosine derivatives) results in a lower interfacial area per head group. The latter will promote a higher packing density of the hydrocarbon chains [23].

As far as the lateral packing is concerned, some very interesting features are observed. The present study clearly shows that the CER head group architecture affects the lateral organization in equimolar CER:CHOL:FFA mixtures (Fig. 7). At 20 °C, the scissoring contour in the FTIR spectrum of the equimolar mixture containing phytoCER shows a clear presence of hexagonal domains. This contrasts the observations in the FTIR spectra of the equimolar mixtures prepared from sphingoCER and non-hydroCER, in which a more predominant orthorhombic packing is observed. This is also in excellent agreement with studies by Rerek et al. [23]. They reported a hexagonal chain packing of the pure phytosphingosine derived CER, compared to the pure sphingosine derived CER and suggest that the absence of an –OH-group at the fourth position of the base chain allows the sphingosine CER to tightly pack into an orthorhombic phase. In addition, for pure substances, a similar phenomenon is observed when comparing sphingosine derived CER to an α-hydroxy or non-hydroxy fatty acid. The former has an additional hydroxyl group at the fatty acid chain and forms a predominant hexagonal packing at room temperature [26]. It seems that the pure sphingosine and phytosphingosine derivatives reveal a very similar lateral packing, whether or not CER is present as pure component or in a complex mixture with CHOL and FFAs. This may to a certain extent be surprising as Dahlen and Pascher [48] showed that in pure CER systems one of the crystal lattices is in a splayed chain conformation resulting in a dense packing of the chains. When we compare the lateral packing of the single CER to the various synthetic CER mixtures in absence of CHOL and FFA, the synCER mixture does not show a splitting in the scissoring and rocking modes, whereas the splitting of the non-hydroCER and sphingoCER is only minor, even after a long equilibration time (more than 72 h). The reduced splitting in these more complex CER mixtures might be due to the variation in head group architecture and chain-length distribution.

The mixtures containing sphingoCER, phytoCER or non-hydroCER (Fig. 7) all show doublet CH_2 scissoring contours in the spectrum until around 58 °C compared to 40 °C in the equimolar synCER:CHOL:FFA mixture (Fig. 3). Studies in which FFAs were replaced by DFFAs revealed only a weak splitting of the CD_2 scissoring vibrations for the sphingoCER or non-hydroCER containing mixtures which disappears almost completely between 20 °C and 40 °C, similarly as in the synCERs containing mixtures. This suggests that a reduction in CER components to only 3 does not affect the mixing properties between FFA and CER and that the orthorhombic phase at elevated temperatures is not due to phase separated FFA.

As far as the various phase transitions are concerned, in sphingoCER:CHOL:FFA, phytoCER:CHOL:FFA and non-hydroCER:CHOL:FFA mixtures the disappearance of the orthorhombic lateral packing occurs just before a substantial amount of disordered fluid phase is formed (Fig. 6, starting at around 60 °C). This suggests that a hexagonal packing is formed prior to the transition to the liquid phase.

When focusing on the CH_2 rocking modes in the spectra of the sphingoCER:CHOL:DFFA and non-hydroCER:CHOL:DFFA mixtures at 20 °C, again some interesting features are displayed. The doublet CH_2 rocking mode indicates the presence of an orthorhombic sublattice in these mixtures, showing that besides a hexagonal lateral packing, CER rich domains with orthorhombic packing are formed. This phenomenon was also observed in the synCER:CHOL:DFFA mixtures (Fig. 3c). This observation strongly indicates that DFFAs promote the formation of protonated sphingoCER (or non-hydroCER) rich domains forming an orthorhombic packing. As these mixtures form the LPP, the same mechanisms can be suggested for the formation of these domains with orthorhombic packing as provided for the synCER:CHOL:DFFA mixtures (see above).

When extrapolating the findings reported in this study to the lipid phase behavior in SC, a few important conclusions can be drawn. The synCER:CHOL:FFA mixtures closely resemble the phase behavior in human SC and in hCER:CHOL:FFA mixtures. Therefore, the synCER containing mixtures form an excellent tool for the detailed study of the effect of changes in lipid composition on the lipid phase behavior. In the present study it has clearly been demonstrated that the linoleate moiety of CER1 shows a conformational disordering, similar to that in a liquid phase. In addition, the CER and FFA participate in the same lattice. However, also FFA rich and synCER rich domains are formed, most probably within the lipid lamellae. Finally, phytosphingosine derived CERs form mainly a hexagonal lattice when mixed with CHOL and FFAs. This is different from the sphingosine derived and non-hydroxy derived CERs. This might have implications for diseased skin, in which often an altered CER composition has been encountered [49]. An increase in the level of phytosphingosine based CER in diseased skin may promote the formation of the hexagonal lateral packing. Therefore, a balanced CER composition may be crucial for a proper lipid organization mimicking the human SC.

Acknowledgements

We would like to thank the company Cosmoferm B.V. for the provision of the synthetic ceramides. The Netherlands Organization for Scientific Research (NWO) is acknowledged for the provision of the beam time and we thank the personnel at the DUBBLE beam line 26 at the ESRF for their support with the X-ray measurements. We like to thank Dr J. Thewalt for the excellent discussions on the interpretations of the conformation disordering of the linoleate moiety of CER1.

References

[1] O. Simonetti, J.A. Hoogstrate, W. Bialik, J.A. Kempenaar, A.H.G.J. Schrijvers, H.E. Bodde, M. Ponec, Visualization of diffusion pathways across the stratum corneum of native and in vitro reconstructed epidermis by confocal laser scanning microscopy, Arch. Dermatol. Res. 287 (1995) 465–473.
[2] M.E.M.J. Meeuwissen, J. Janssen, C. Cullander, H.E. Junginger, J.A. Bouwstra, A cross-section device to improve visualization of fluorescent probe penetration into skin by confocal laser scanning microscopy, Pharm. Res. 15 (1998) 352–356.
[3] K.C. Madison, D.C. Swarzendruber, P.W. Wertz, D.T. Downing, The biochemistry and function of stratum corneum, J. Invest. Dermatol. 90 (1998) 110–116.
[4] J.A. Bouwstra, G.S. Gooris, M.A. Salomons-de Vries, J.A. van der Spek, W. Bras, Structure of human stratum corneum as function of temperature and hydration: a wide angle X-ray diffraction study, Int. J. Pharm. 84 (1992) 205–216.
[5] P.W. Wertz, D.T. Downing, Epidermal lipids, in: L.A. Goldsmith (Ed.), Physiology, Biochemistry and Molecular Biology of the Skin, 2nd edn, Oxford University Press, 1991, pp. &!#32205–236.
[6] M. Ponec, P. Lankhorst, A. Weerheim, P. Wertz, New acylceramide in native and reconstructed epidermis, J. Invest. Dermatol. 120 (2003) 581–588.
[7] M.W. De Jager, G.S. Gooris, I.P. Dolbnya, W. Bras, M. Ponec, J.A. Bouwstra, Novel lipid mixtures based on synthetic ceramides reproduce the unique stratum corneum lipid organization, J. Lipid Res. 45 (2004) 923–932.
[8] G.S. Gooris, J.A. Bouwstra, Infrared spectroscopic study of stratum corneum model membranes prepared from human ceramides, cholesterol and fatty acids, Biophys. J. 92 (2007) 2785–2795.
[9] C.N. Laugel, Yagoubi, A. Baillet, ATR–FTIR spectroscopy: a chemometric approach for studying the lipid organization of the stratum corneum, Chem. Phys. Lipids 135 (2005) 55–68.
[10] G.S.K. Pilgram, A.M. Engelsma-van Pelt, J.A. Bouwstra, H.K. Koerten, Electron diffraction provides new information on human stratum corneum lipid organization studies in relation to depth and temperature, J. Invest. Dermatol. 113 (1999) 403–409.
[11] J.A. Bouwstra, G.S. Gooris, F.E.R. Dubbelaar, M. Ponec, Phase behavior of lipid mixtures based on human ceramides: coexistence of crystalline and liquid phases, J. Lipid Res. 42 (2001) 1759–1770.
[12] M.W. De Jager, G.S. Gooris, I.P. Dolbnya, M. Ponec, J.A. Bouwstra, The phase behaviour of skin lipid mixtures based on synthetic ceramides, Chem. Phys. Lipids 124 (2003) 123–134.
[13] M.W. De Jager, G.S. Gooris, M. Ponec, J.A. Bouwstra, Lipid mixtures prepared with well-defined synthetic ceramides closely mimic the unique stratum corneum lipid phase behavior, J. Lipid Res. 46 (2005) 2649–2656.
[14] J.A. Bouwstra, F.E.R. Dubbelaar, G.S. Gooris, M. Ponec, The lipid organisation in the skin barrier, Acta Derm.-Venereol., Suppl. 208 (2000) 23–30 (Stockh.).

[15] B. Ongpipattanakul, M.L. Francoeur, R.O. Potts, Polymorphism in stratum corneum lipids, Biochim. Biophys. Acta 1190 (1994) 115–122.
[16] D. Bommannan, R.O. Potts, R. Guy, Examination of stratum corneum barrier function in vivo by infrared spectroscopy, J. Invest. Dermatol. 95 (1990) 403–408.
[17] J.A. Bouwstra, G.S. Gooris, F.E.R. Dubbelaar, A. Weerheim, M. Ponec, pH and cholesterol sulfate and fatty acids affect the stratum corneum lipid organisation, J. Invest. Dermatol., Symp. Proc. 3 (1998) 69–74.
[18] J. Thewalt, N. Kitson, C. Araujo, A. MacKay, M. Bloom, Models of stratum corneum intercellular membranes: the sphingolipid headgroup is a determinant of phase behavior in mixed lipid dispersions, Biochem. Biophys. Comm. 188 (1992) 1247–1252.
[19] N. Kitson, J. Thewalt, M. Lafleur, M. Bloom, A model membrane approach to the epidermal permeability barrier, Biochemistry 33 (1994) 6707–6715.
[20] R.A. Demel, B. de Kruyff, The function of sterols in membranes, Biochim. Biophys. Acta 457 (1976) 109–132.
[21] F. Liu, I.P. Sugar, P.L.G. Chong, Cholesterol and ergosterol superlattices in three component liquid crystalline lipid bilayers as revealed by dehydroergosterol fluorescence, Biophys. J. 72 (1997) 2243–2254.
[22] S.M. Motta, M. Monti, S. Sesana, R. Caputo, S. Carelli, R. Ghidoni, Ceramide composition of psoriatic scale, Biochim. Biophys. Acta 1182 (1993) 147–151.
[23] M.E. Rerek, H. Chen, B. Markovic, D. van Wyck, P. Garidel, R. Mendelsohn, D.J. Moore, Phytosphingosine and sphingosine ceramide headgroup hydrogen bonding: structural insights through thermotropic hydrogen/deuterium exchange, J. Phys. Chem., B. 105 (2001) 9355–9363.
[24] D.J. Moore, M.E. Rerek, Insights into the molecular organization of lipids in the skin barrier from infrared spectroscopy studies of stratum corneum lipid models, Acta Derm.-Venereol., Suppl. 208 (2000) 16–22.
[25] D.J. Moore, M.E. Rerek, R. Mendelsohn, FTIR spectroscopy studies of the conformational order and phase behavior of ceramides, J. Phys. Chem., B. 101 (1997) 8933–8940.
[26] M.E. Rerek, D. van Wyck, R. Mendelsohn, D.J. Moore, FTIR spectroscopic studies of lipid dynamics in phytosphingosine ceramide models of the stratum corneum lipid matrix, Chem. Phys. Lipids 134 (2005) 51–58.
[27] D.J. Moore, M.E. Rerek, R. Mendelsohn, Lipid domains and orthorhombic phases in model stratum corneum: evidence from Fourier transform infrared spectroscopy studies, Biochem. Biophys. Res. Comm. 231 (1997) 797–801.
[28] J.A. Bouwstra, G.S. Gooris, K. Cheng, A. Weerheim, W. Bras, M. Ponec, Phase behaviour of isolated skin lipids, J. Lipid Res. 37 (1996) 999–1011.
[29] I.P. Dolbnya, H. Alberda, F.G. Hartjes, F. Udo, R.E. Bakker, M. Konijnenburg, E. Homan, I. Cerjak, P. Goedtkindt, W. Bras, A fast position sensitive MSGC detector at high count rate operation, Rev. Sci. Instrum. 73 (2002) 3754–3758.
[30] R. Mendelsohn, G.L. Liang, H.L. Strauss, R.G. Snyder, IR spectroscopic determination of gel state miscibility in long-chain phosphatidylcholine mixtures, Biophys. J. 69 (1995) 1987–1998.
[31] V. Velkova, M. Lafleur, Influence of lipid composition on the organization of skin lipid model membranes: an infrared spectroscopy investigation, Chem. Phys. Lipids 117 (2002) 63–74.
[32] H.C. Chen, R. Mendelsohn, M.E. Rerek, D.J. Moore, Effect of cholesterol on miscibility and phase behaviour in binary mixtures with synthetic ceramide 2 and octadecanoic acid Infrared studies, Biochim. Biophys. Acta 1512 (2001) 345–356.
[33] X. Chen, S. Kwak, M. Lafleur, M. Bloom, N. Kitson, J. Thewalt, Fatty acids influence "solid" phase formation in models of stratum corneum intercellular membranes, Langmuir 23 (2007) 5548–5556.
[34] S.H. White, D. Mirejovsky, G.I. King, Structure of lamellar lipid domains and corneocyte envelopes of murine stratum corneum. An X-ray diffraction study, Biochemistry 27 (1988) 3725–3732.
[35] J.A. Bouwstra, G.S. Gooris, J.A. van der Spek, W. Bras, Structural investigations on human stratum corneum by small angle X-ray scattering, J. Invest. Dermatol. 97 (1991) 1005–1012.
[36] R.G. Snyder, M.C. Goh, V.J.P. Srivatsavoy, H.L. Strauss, D.L. Dorset, Measurement of the growth kinetics of microdomains in binary *n*-alkane solid solutions by infrared spectroscopy, J. Phys. Chem. 96 (1992) 10008–10019.
[37] E. Ten Grotenhuis, R.A. Demel, M. Ponec, D.R. de Boer, J.C. van Miltenburg, J.A. Bouwstra, Phase behaviour of stratum corneum lipids in mixed Langmuir blodgett monolayer, Biophys. J. 7 (1996) 1389–1399.
[38] A.C.T. Texeira, A.C. Fernandes, A.R. Garcia, L.M. Ilharco, P. Brogueira, A.M.P.S. Goncalves da Silva, Microdomains in mixed monolayers of oleanolic and stearic acids: thermodynamic study and BAM observation at the air–water interface and AFM and FTIR analysis of LB monolayers, Chem. Phys. Lipids 149 (2007) 1–13.
[39] L. Scheffer, I. Solomonov, M. van Weynand, K. Kjaer, L. Leiserowitz, L. Addadi, Structure of cholesterol/ceramide monolayer mixtures: implications to the molecular organisation of lipid rafts, Biophys J. 88 (2005) 3381–3391.
[40] J.A. Bouwstra, G.S. Gooris, F.E.R. Dubbelaar, A.M. Weerheim, A.P. IJzerman, M. Ponec, The role of ceramide 1 in the molecular organization of the stratum corneum lipids, J. Lipid Res. 39 (1998) 186–196.
[41] T.J. McIntosh, M. Stewart, D.T. Downing, X-ray diffraction analysis of isolated skin lipids: reconstitution of intercellular lipid domains, Biochemistry 35 (1996) 3649–3653.
[42] J.A. Bouwstra, G.S. Gooris, F.E.R. Dubbelaar, M. Ponec, Phase behaviour of lipid mixtures based on human ceramides: the role of natural and synthetic ceramide 1, J. Invest. Dermatol. 118 (2002) 606–616.
[43] V. Schreiner, G.S. Gooris, G. Lanzendörfer, S. Pfeiffer, H. Wenck, W. Diembeck, E. Proksch, J.A. Bouwstra, Barrier characteristics of different human skin types investigated with X-ray diffraction, lipid analysis and electron microscopy imaging, J. Invest. Dermatol. 114 (2000) 654–660.
[44] M.W. De Jager, G.S. Gooris, M. Ponec, J.A. Bouwstra, Acylceramide head group architecture affects lipid organization in synthetic ceramide mixtures, J. Invest. Derm. 123 (2004) 911–916.
[45] M.W. De Jager, H.W.W. Groenink, R. Bielsa i Guivernau, E.E. Andersson, N.S. Angelova, M. Ponec, J.A. Bouwstra, A novel in vitro percutaneous penetration model: evaluation of barrier properties with p-aminobenzoic acid and two of its derivatives, Pharm. Res. 23 (2006) 951–960.
[46] B. Forslind, A domain mosaic model of the skin barrier, Acta Derm.-Venereol. 74 (1994) 1–6.
[47] L. Norlen, Skin barrier structure and function: the single gel phase model, J. Invest. Dermatol. 117 (2001) 830–836.
[48] B. Dahlen, I. Pascher, Molecular arrangement in sphingolipids. Thermotropic phase behaviour of tetracosanoylphytosphingosine, Chem. Phys. Lipids 24 (1979) 119–133.
[49] J.A. Bouwstra, M. Ponec, The skin barrier in healthy and diseased state, Biochim. Biophys. Acta 1758 (2006) 2080–2095.